

A Numerical Study of Line-Edge Roughness in Graphene Superlattice-Based Photodetectors

M. Moradinasab^{†*}, M. Pourfath^{†*}, M. Fathipour[†], and H. Kosina^{*}

^{*}Institute for Microelectronics, TU Wien, Gußhausstraße 27–29/E360, 1040 Wien, Austria

[†]Department of Electrical and Computer Engineering, University of Tehran, Tehran, Iran

e-mail: moradinasab@iue.tuwien.ac.at

Abstract—In this work we show that superlattices formed as segments of armchair graphene nanoribbons (AGNRs) with periodically modulated widths can be used as infra-red photodetectors. Based on the nonequilibrium Green's function formalism, along with an atomistic tight-binding model, the optical characteristics of AGNR-based hydrogen-terminated and boron nitrogen-terminated superlattices are studied. The role of line-edge roughness on the optical properties of such devices is carefully studied.

I. INTRODUCTION

Graphene, a zero band gap material, has attracted considerable attention from the scientific community due to its excellent electronic, optoelectronic, and spintronic properties [1]. In order to use graphene in electronic applications, a gap should be induced. Confining graphene in one dimension is the most common approach to achieve a band gap. Based on this approach, graphene nanoribbons (GNRs) have been introduced where graphene sheets are patterned into narrow ribbons. The band gap in GNRs is inversely proportional to the width of nanoribbons.

It was suggested that superlattices formed as segments of armchair GNRs (AGNRs) with periodically modulated widths can be fabricated and optimized for different electronic and photonic applications [2]. A recent experimental work indicates the feasibility of fabricating graphene nanoribbons with different widths, which can be considered as segments of a superlattice based on GNRs [3]. Such structures can behave as multiple quantum well structures and exhibit interesting quantum effects such as resonant tunneling [4]. However, for such narrow structures, line-edge roughness plays an important role on the device characteristics [5].

To date, many theoretical works have investigated the GNRs analytically [6] and numerically [5] and several groups have studied graphene-based superlattices [7]. In this work we show that superlattices formed as segments of AGNRs with periodically modulated widths can be used as infra-red photodetectors. The optical properties of AGNR-based hydrogen-terminated (HSL) and boron nitrogen-terminated (BNSL) superlattices, are investigated. The effect of line-edge roughness on the optical properties of such photodetector devices is carefully studied.

II. METHODS

Over the past decade the non-equilibrium Green's function formalism has been widely employed to investigate various

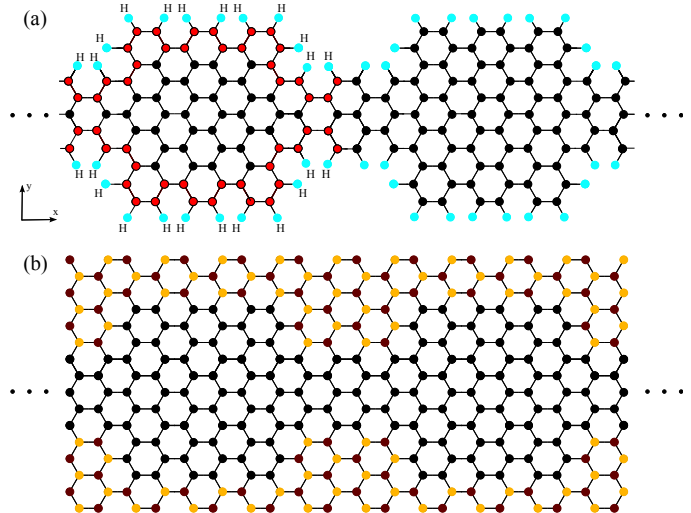


Fig. 1. Sketch of (a) an HSL(11) and (b) a BNSL(11) photodetectors. Edge carbon atoms are saturated by hydrogen and boron nitrogen atoms, respectively.

nano electronic devices [10]. In this formalism the effect of various interactions is included in the self-energy term:

$$G(E) = [(E + i0^+)I - H - \Sigma_1 - \Sigma_2 - \Sigma_s]^{-1} \quad (1)$$

where H is the Hamiltonian matrix. Σ_1 and Σ_2 are the self-energies of the left/right contacts and Σ_s is the scattering self-energy, respectively. The NEGF formalism is employed to simulate the photoconductivity of graphene superlattice-based photodetector devices. The Hamiltonian of the electron-photon interaction can be written as [2], [8]:

$$\hat{H}_{e-ph} = \sum_{\langle l,m \rangle} M_{l,m} (\hat{b}e^{-i\omega t} + \hat{b}^\dagger e^{i\omega t}) \hat{a}_l^\dagger \hat{a}_m \quad (2)$$

$$M_{l,m} = (z_m - z_l) \frac{ie}{\hbar} \sqrt{\frac{\hbar I_\omega}{2N\omega\epsilon c}} \langle l | \hat{H}_0 | m \rangle \quad (3)$$

where z_m denotes the position of the carbon atom at site m , I_ω is the photon flux with the frequency ω , and N is the photon population number. The incident light is assumed to be monochromatic, with polarization along the longitudinal axis, see Fig. 1.

III. RESULTS AND DISCUSSIONS

Fig. 2 compares the optical characteristics and bandstructures for HSL(11) and BNSL(11). Carbon-carbon interactions

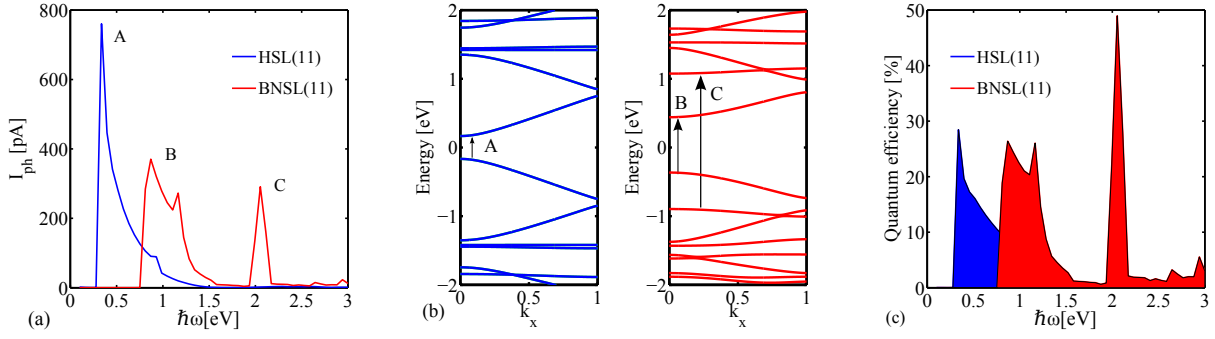


Fig. 2. Photocurrent spectrum and electronic band structure for HSL(11) and BNSL(11) photodetectors.

up to three nearest neighbors are considered in tight-binding calculations for HSLs. In the case of the BNSL structures, a more careful choice of the TB parameters is required due to a change of ionicities of the boron and nitrogen atoms at the edges of the superlattice with respect to that of a nanoribbon. We propose the tight-binding parameters which are in excellent agreement with first-principle simulations. Using these tight binding parameters, as shown in Fig. 2-b, larger energy gap is achieved for BNSL(11) compared to HSL(11). This difference in the bandgap is attributed to the large ionic potential difference between the B and N atoms in BNSLs.

To assess the performance of superlattice structures for photodetection applications, the quantum efficiency and photoresponsivity of the presented structures are evaluated. The quantum efficiency is defined as $\alpha = (I_{ph}/q)/(P_{op}/\hbar\omega)$, where I_{ph} and P_{op} are the photocurrent and the incident optical power, respectively. The quantum efficiency peaks whenever the photon energy corresponds to an allowed intersubband optical transition. Efficiency reaches 27% to 28% in HSLs. For the case of BNSLs, as expected, there are more peaks in the specified energy range due to the changes in subband spacings of the bandstructure. The peak photoresponsivities, defined as I_{ph}/P_{op} , of HSL and BNSL are calculated as 0.86 A/W and 0.33 A/W, where the optical power of the incident photons is assumed to be 10^5 W/cm².

Line-edge roughness effects play an important role in graphene narrow structures. The effect of line-edge roughness on the electronic properties of GNRs has been investigated in several analytical [11] and numerical [12] studies. Here, we investigate the role of roughness on the spectrum of photocurrent in GNR-based superlattices using statistical anal-

ysis. For the given geometrical and roughness parameters many samples are statistically generated. The characteristics of each device is evaluated followed by an ensemble average over all samples. Figure 3 exhibits the results for HSL(11) and BNSL(11) with edge disorders. Due to backscattering of carriers, the photocurrent and quantum efficiencies of both superlattices decrease in the presence of line-edge roughness. Figure 3 shows that due to effective width variation, the photoabsorption peaks appear at energies larger or smaller than the peaks of the structure without disorder. The average width of edge-defected devices, however, is equal to that of a device with perfect edges. Therefore, line-edge roughness does not affect the location of the photocurrent peak. The average photocurrent of edge-defected HSL peaks at photon energies around $\hbar\omega = 1$ eV. This peak is related to midgap states induced by line-edge roughness. Due to the formation of dangling bonds in the presence of line-edge roughness, midgap states are formed. In the case of GNR-based transistors such states result in significant increase of the off-current. However, dangling bonds are absent in edge-defected BNSLs and midgap states do not appear in such structures. HSL(11) exhibits photoresponsivity and quantum efficiency reductions of 23%, 55%, and 70% for the relative roughness amplitudes of 3%, 4%, and 5%, respectively, whereas a smoother behavior is observed for BNSL(11). This behavior is attributed to the stable configuration of edge-carbon atoms in BNSLs comparison with HSLs in the presence of line-edge roughness.

ACKNOWLEDGMENT

This work has been supported in parts by the Austrian Science Fund FWF through grant F2514, and the European Communitys Seventh Framework Programme, grant FP7-263306.

REFERENCES

- [1] P. Avouris *et al.*, Nature Photonics, **2**, 341 (2008).
- [2] L. E. Henrickson, J. Appl. Phys., **91**, 6273 (2002).
- [3] X. Li *et al.*, Science, **319**, 1229 (2008).
- [4] H. Teong *et al.*, J. Appl. Phys., **105**, 084317 (2009).
- [5] A. Y. Goharrizi *et al.*, Trans. Elect. Dev. **59**, 3527 (2012).
- [6] M. Moradinasab *et al.*, J. Appl. Phys., **111**, 074318 (2012).
- [7] M. Topsakal *et al.*, Appl. Phys. Lett., **92**, 173118 (2008).
- [8] D. A. Stewart *et al.*, Phys. Rev. Lett **4**, 107401 (2004).
- [9] D. Gunlycke *et al.*, Phys. Rev. B, **77**, 115, (2008).
- [10] W. Zou *et al.*, Appl. Phys. Lett., **100**, 103109, (2012).
- [11] A. Y. Goharrizi *et al.*, Trans. Elect. Dev. **58**, 3725 (2012).
- [12] M. Evaldsson *et al.*, Phys. Rev. B, **78**, 161407, (2008).

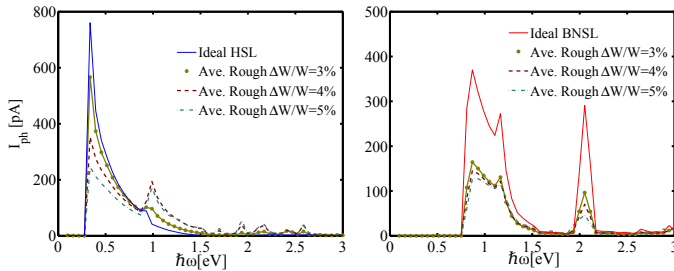


Fig. 3. Photocurrent spectrum with different roughness amplitudes for (a) HSL(11) and (b) BNSL(11).